TABLE 5 Antenna Characteristics (UC: Unit Cells, ES: Electrically Size, PHS: Physically Size)

Papers	Dimensions	Bandwidth	Gain (Max)	Efficiency (Max)
[8] b-shaped antenna with 4 UC	ES: $0.047\lambda_0 \times 0.021\lambda_0 \times 0.002\lambda_0$ at 1 GHz PHS: $14.2 \times 6.32 \times 0.8$ mm^3	1–3.2 GHz (104.76%)	2.3 dBi	62%
[8] b-shaped antenna with 6 UC	ES: $0.051\lambda_0 \times 0.016\lambda_0 \times 0.002\lambda_0$ at 800 MHz PHS: $19.2 \times 6.32 \times 0.8$ mm^3	0.8–3.4 GHz (123.8%)	2.8 dBi	70%
[9] J-shaped antenna with 8 UC	ES: $0.564\lambda_0 \times 0.175\lambda_0 \times 0.02\lambda_0$ at 7.5 GHz PHS: $22.6 \times 7 \times 0.8$ mm^3	7.25–17.8 GHz (84.23%)	2.35 dBi	48.2%
[9] I-shaped antenna with 7 UC	ES: $0.556\lambda_0 \times 0.179\lambda_0 \times 0.041\lambda_0$ at 7.7GHz PHS: $21.7 \times 7 \times 1.6$ mm^3	7.8–19.85 GHz (87.16%)	3.4 dBi	68.1%
Proposed E-shaped antenna with 2 UC	ES: $0.017\lambda_0 \times 0.006\lambda_0 \times 0.001\lambda_0$ at 500 MHz PHS: $10.2 \times 3.9 \times 0.8$ mm^3	0.5–1.35 GHz (91.89%)	5.3 dBi	85%
Proposed E-shaped antenna with 3 UC	ES: $0.028\lambda_0 \times 0.008\lambda_0 \times 0.001\lambda_0$ at 650 MHz PHS: 1 $3.2 \times 3.9 \times 0.8$ mm^3	0.65–1.85 GHz (96%)	5.7 dBi	90%

boards. The proposed antennas have advantages of small size, wide bandwidth, high gains and efficiencies, isotropic radiation patterns, low profile, light weight, low cost, and ease of implementation.

ACKNOWLEDGMENTS

The author would like to express his sincere thanks to the Microelectronic Research and Development Center of Iran (MERDCI), the microwave and millimeter wave laboratory of the Amirkabir University of Technology (Tehran Polytechnic), Tehran, Iran and the antenna laboratory of the K. N. Toosi University of Technology, Tehran, Iran for supporting this work and providing the experimental data.

REFERENCES

1. R.W. Ziolkowski and A.D. Kipple, Application of double negative materials to increase the power radiated by electrically small antennas, IEEE Trans Antennas Propag 51 (2003), 2626–2640.
2. G.V. Eleftheriades, A. Grbic, and M. Antoniades, Negative-refractive-index transmission-line metamaterials and enabling electromagnetic applications, In: IEEE Antennas and Propagation Society International Symposium, Monterrey, CA, 2004, pp. 1399–1402.
3. M. Alibakhshi-Kenari, Design and modeling of new UWB metamaterial planar cavity antennas with shrinking of the physical size for modern transceivers, Int J Antennas Propag 2013 (2013), 12 pages, Article ID 562538. doi:10.1155/2013/562538.
4. M. Alibakhshi-Kenari, M. Movahhedi, and H. Naderian, A new miniature ultra wide band planar microstrip antenna based on the metamaterial transmission line, In: 2012 IEEE Asia- Pacific Conference on Applied Electromagnetics (APACE 2012), Melaka, Malaysia, 2012, pp. 293–297.
5. M. Alibakhshi-kenari and M. Naser-Moghadasi, A novel CRLH-CP antenna with the capability to be integration inside RF components for RF electronic devices and embedded systems, J Appl Comput Electromagn Soc (ACES J), in press.
6. C.J. Lee, M. Achour, and A. Gummalla, Compact metamaterial high isolation MIMO antenna subsystem, In: 2008 Asia Pacific Microwave Conference, Macau, 2008, pp. 1–4.
7. C.J. Lee, K.M.H. Leong, and T. Itoh, Broadband small antenna for portable wireless application, In: International Workshop on Antenna Technology: Small Antennas and Novel Metamaterials iWAT 2008, Chiba, 2008, pp. 10–l 3.
8. M. Alibakhshi-Kenari, Printed planar patch antennas based on metamaterial, Int J Electron Lett 2 (2014), 37–42.
9. M. Alibakhshi-Kenari, Introducing the new wideband small plate antennas with engraved voids to form new geometries based on CRLH MTM-TLs for wireless applications, Int J Microwave Wireless Technol 6 (2014), 629–637.

NOVEL 3D PRINTED SYNTHETIC DIELECTRIC SUBSTRATES

Shiyu Zhang, Chinwe C. Njoku, William G. Whittow, and John C. Vardaxoglou

School of Electronic, Electrical and Systems Engineering, Loughborough University, Epinal Way, Loughborough, Leicestershire LE11 3TU, United Kingdom; Corresponding author: s.zhang@lboro.ac.uk

Received 18 March 2015

ABSTRACT: *This letter presents dielectric properties of air filled synthetic substrates fabricated in a single process using three-dimensional printing. The permittivity and loss tangent of a given sized substrate can be changed by controlling the air infill volume fraction.* © 2015 The Authors. Microwave Opt Technol Lett 57:2344–2346, 2015; View this article online at wileyonlinelibrary.com. DOI 10.1002/mop.29324

Key words: *3D printing; synthetic materials; dielectric substrates*

1. INTRODUCTION

Additive manufacturing (AM) technology constructs successive layers of materials to create three-dimensional (3D) objects. With computer aided design (CAD) and computer aided manufacturing (CAM), it is possible to build rapid prototypes in almost any geometry and internal structure. The advances in digital AM equipment and new materials enables 3D printing to produce a wide range of products in a variety of fields including biology, aerospace, electronics, and electromagnetics (EM) [1–5].

There are a number of EM applications that require complicated shapes and 3D internal structures, such as lens antennas and metamaterials, to achieve bespoke EM properties. Traditional mechanical machining and micromachining have been up to now the dominant approach for fabrication [6,7]. These machining techniques remove or shape parts of raw materials using operations such as drilling and milling. This is time costly and also generates material wastage. Moreover, it is difficult to create complicated internal structures using machining techniques in a single process. With 3D printing, the final shape is successively constructed layer by layer and machining is not required. Therefore, there is no waste of materials for 3D printing, and it is easy to generate complicated internal structures. 3D printed dielectric materials which are cost efficient and can be rapidly prototyped are becoming increasingly attractive in antenna design and fabrication.

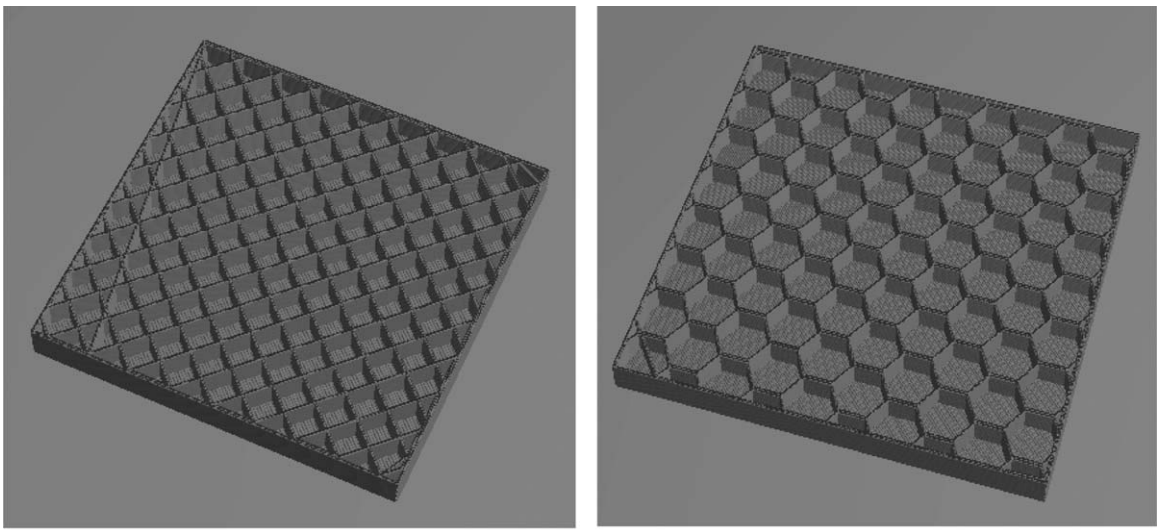

Figure 1 CAD sketch of different internal structures of 3D printed dielectric substrates (top lids are not shown). [Color figure can be viewed in the online issue, which is available at wileyonlinelibrary.com] (a) Waffle infill and (b) honeycomb infill.

The specifications of dielectric laminates, such as thickness and relative permittivity, are usually determined by the manufacturers, and therefore, antenna engineers' designs are restricted. Using 3D printing in dielectric materials, fabrication allows engineers to customize the substrate to desired dimensions, for instance, conformal antenna applications. Furthermore, using 3D printing can create multiple-material objects in a single process which means assembly is not required. Therefore, it is much easier to produce synthetic dielectric materials with combinations of diverse materials such as plastics, polymers, nylons, and ceramics using 3D printing. This letter demonstrates the combination of nontoxic material polylactic acid (PLA) and air to spawn novel dielectric substrates. The dielectric properties of materials such as permittivity and loss factor can be tailored with different air to PLA percentage ratios.

2. 3D PRINTED DIELECTRIC SUBSTRATES

In this work, a fused deposition modeling (FDM) Makerbot® Replicator™ 2X 3D printer was used to print the dielectric substrate samples. The 3D models were designed using CAD tools and subsequently sliced into successive layers. The heated printer nozzle extruded the thermal material and created the object layer by layer from the bottom upwards. Each layer thickness was 0.2 mm, and the extrusion temperature of the printer nozzle for the PLA material was 200°C.

The 3D printed substrates were constructed of three parts: top lid, bottom base, and the nonsolid infill pattern in the middle. The lid and base were printed using 100% infill PLA. The middle part was printed with various infill patterns with air voids. Three internal infill structures including waffle, honeycomb, and empty were used here for examining the effect of infill patterns on the dielectric properties. Figure 1 shows the CAD models of the waffle and honeycomb lattice infill patterns. To reveal the internal structures, the top lids are not shown. The waffle infill is shown in in Figure 1(a). The vertical interior walls were at 45° angles in relation to the outer walls. Figure 1(b) shows the honeycomb infill pattern. The internal and exterior wall thicknesses of both waffle and honeycomb were 0.4 mm. After, the top lids were printed all the samples had the same external dimensions: 50 mm × 50 mm × 2.4 mm. The cross section of the substrate is shown in Figure 2. A structural layer thickness of 0.8 mm (made up from four 0.2-mm PLA layers) was chosen to produce an overall thickness of 2.4 mm. An empty sample of the same overall thickness was also printed for comparison. The thicknesses of the lid and base of the empty infill sample were both 0.4 mm.

The infill percentage indicated the PLA volume fraction (VF) which was the volume ratio of PLA material to the whole printed sample, excluding the four exterior walls. The PLA VF for a solid substrate was 100%. The VF was varied by changing the infill patterns. Smaller patterns resulted in higher PLA VF. The PLA VF included the top lid and bottom base. Thus, the hollow infill sample had 33% PLA VF.

3. RESULTS

Six dielectric substrate samples were printed. A commercially available, split postdielectric resonator from QWED (www.qwed.com.pl) was used for measuring the relative permittivity and loss tangent of these samples at 2.4 GHz [8]. The details of the infill structure and measured results are shown in Table 1. Sample A with 100% infill had a measured permittivity of 2.72 and loss tangent of 0.008. Both samples B and C used waffle infill with different PLA VF. The waffle squares in sample B were smaller than sample C and, therefore, sample B had higher PLA VF. A larger PLA volume showed an increase in both permittivity and loss tangent. Sample D had the same PLA volume fraction as sample C but used the honeycomb infill. The

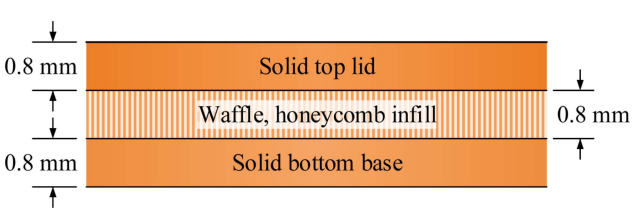

Figure 2 Cross section view of 3D printed nonsolid dielectric substrates. [Color figure can be viewed in the online issue, which is available at wileyonlinelibrary.com]

TABLE 1 Measured Dielectric Properties of 3D Printed Samples With 2.4 mm Thickness at 2.4 GHz

Sample	Infill Pattern	PLA VF	Relative Permittivity	Loss Tangent
A	Solid	100%	2.72	0.008
B	Waffle	73%	2.53	0.008
C	Waffle	70%	2.27	0.006
D	Honeycomb	70%	2.25	0.006
E	No infill (empty)	33%	1.60	0.004
F	Honeycomb (0.2-mm base, without lid)	18%	1.24	0.002

measured results indicated that the infill shape did not greatly affect the dielectric properties.

Although sample E had no infill, the inclusion of the lid and base made up 33% of the total volume. To examine the effects of the external walls, sample F was printed with the same honeycomb infill with thinner bottom base but without the top lid. The thicknesses of the base and the honeycomb infill part of sample F were 0.2 mm and 2.2 mm, respectively. The measured results showed that sample F had a lower permittivity and loss tangent value than sample E, due to its lower PLA volume fraction.

4. CONCLUSION

This letter has presented the feasibility of creating low loss dielectric substrates with various relative permittivities and loss tangent values using conventional 3D printing. Voids were introduced inside the substrates which were printed in one process. The volume fraction of air in the host material affected the dielectric properties more significantly than the infill shape. The permittivity and loss factor of the substrate were reduced by the increasing air volume fraction. Therefore, the permittivity and loss tangent of the dielectric substrate can be tailored to the desired values by extrapolating from the sample results produced here.

These highly customisable dielectric materials will improve the flexibility of antenna design and related EM applications. The automatic fabrication process also allows the dielectric properties to be graded within one structure.

REFERENCES

1. S. Bose, S. Vahabzadeh, and A. Bandyopadhyay, Bone tissue engineering using 3D printing, Mater Today 16 (2013), 496–504.
2. E. Macdonald, R. Salas, D. Espalin, M. Perez, E. Aguilera, D. Muse, and R.B. Wicker, 3D Printing for the rapid prototyping of structural electronics, IEEE Access 2 (2014), 234–242.
3. E.E.L. Canelon, A.G. Loapez, R. Chandra, and A.J. Johansson, 3D printed miniaturized UWB antenna for wireless body area network, In: 8th European Conference on Antennas and Propagation (EuCAP), The Hague, The Netherlands, 2014, pp. 3090–3093.
4. A. Bisognin, D. Titz, F. Ferrero, R. Pilard, C.A. Fernandes, J.R. Costa, C. Corre, P. Calascibetta, J. Riviere, A. Poulain, C. Badard, F. Gianesello, C. Luxey, P. Busson, D. Gloria, and D. Belot, 3D printed plastic 60 GHz lens: Enabling innovative millimeter wave antenna solution and system, In: 2014 IEEE MTT-S International Microwave Symposium (IMS), Tampa, FL, 2014, pp. 1–4.
5. J. Tribe, W.G. Whittow, R.W. Kay, and J.C. Vardaxoglou, Additively manufactured heterogeneous substrates for three-dimensional control of local permittivity, Electron Lett 50 (2014), 745–746.
6. L. Schulwitz and A. Mortazawi, A new low loss Rotman lens design using a graded dielectric substrate, IEEE Trans Microwave Theory Tech 56 (2008), 2734–2741.
7. E.A. Navarro, A. Luximon, I.J. Craddock, D.L. Paul, and M. Dean, Multilayer and conformal antennas using synthetic dielectric substrates, IEEE Trans Antennas Propag 51 (2003), 905–908.
8. J. Krupka, Measurements of the complex permittivity of microwave circuit board substrates using split dielectric resonator and reentrant cavity techniques, In: 7th International Conference on Dielectric Materials, Measurements and Applications, Bath, 1996, pp. 21–24.

INNOVATIVE BIT CHANNEL IN DOWNSTREAM PASSIVE OPTICAL NETWORK FRAMES BASED ON REUSING OF BIT SEQUENCES

Pavel Lafata
Faculty of Electrical Engineering, Department of Telecommunication Engineering Technická 2, Czech Technical University in Prague, 166 27 Prague 6, Czech Republic; Corresponding author: Lafatpav@Fel.Cvut.Cz

Received 19 March 2015

ABSTRACT: *In this article, a novel idea of a hidden bit channel established in the downstream passive optical network (PON) frames is proposed. As the downstream frames in time-division multiplexed, PONs are broadcasted and delivered to all active end-point optical network units (ONUs), and this bitstream could be potentially used for creating an additional hidden bit channel containing bits for all ONUs. Therefore, the downstream frames could simply transmit standard information fields and ONU contributions according to the standard PON principles; however, these bits could be also reused multiple times to carry additional data for each ONU in a form of segmented bit sequences spread within the entire bitstream. To establish effective bit channel with positive bit gain, an effective algorithm for addressing its bits is necessary. The most promising bit addressing algorithm is proposed within this article together with the results obtained by its simulations and performance evaluations.* © 2015 Wiley Periodicals, Inc. Microwave Opt Technol Lett 57:2346–2351, 2015; View this article online at wileyonlinelibrary.com. DOI 10.1002/mop.29323

Key words: *bit addressing; bitstream; passive optical networks; security; XG-PON*

1. INTRODUCTION

The passive optical networks (PONs) are now being widely deployed in many countries as their present generation can reach shared transmission rates up to 10 Gbps [1]. The previous types, such as Ethernet PON (EPON) and Gigabit PON (GPON) according to the IEEE 802.3ah standard [2] and ITU-T G.984 recommendation [3], are currently being replaced by updated PON solutions, 10GEPON presented within IEEE 802.3av std. [4] and XG-PON in ITU-T G.987 [5] rec. All these PON types mentioned above are based on time-division multiplex (TDM) principle while both upstream and downstream TDM frames consist of multiple contributions to/from all active end-points optical network units (ONUs) [6]. Therefore, a part of the optical distribution network (ODN) is always shared by multiple ONUs. The continuous evolution of new PON generations and the progress of their development in the future is now pointed toward applying wavelength multiplexing techniques [7,8], various modulation formats [9], optical code multiplexing [10], and so forth.

The ODN in case of pure PONs is always passive; therefore, the downstream optical signals are split by passive optical